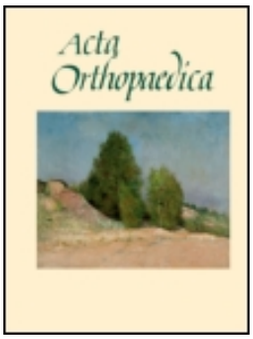

Acta Orthopaedica

ISSN: 1745-3674 (Print) 1745-3682 (Online) Journal homepage: informahealthcare.com/journals/iort20

Local delivery of a selective androgen receptor modulator failed as an anabolic agent in a rat bone marrow ablation model

Hannu T Aro, Julia Kulkova, Niko Moritz, Esa Kähkönen & Riina H Mattila

To cite this article: Hannu T Aro, Julia Kulkova, Niko Moritz, Esa Kähkönen & Riina H Mattila (2015) Local delivery of a selective androgen receptor modulator failed as an anabolic agent in a rat bone marrow ablation model, Acta Orthopaedica, 86:6, 751-759, DOI: 10.3109/17453674.2015.1074840

To link to this article: https://doi.org/10.3109/17453674.2015.1074840

Local delivery of a selective androgen receptor modulator failed as an anabolic agent in a rat bone marrow ablation model

Hannu T ARO[1,3], Julia KULKOVA[1], Niko MORITZ[1,2], Esa KÄHKÖNEN[3], and Riina H MATTILA[1]

[1] Orthopaedic Research Unit, Department of Orthopaedic Surgery and Traumatology, University of Turku and Turku University Hospital, Turku; [2] Turku Clinical Biomaterials Centre, Institute of Dentistry, University of Turku, Turku; [3] Turku University Hospital, Turku, Finland.
Correspondence: hannu.aro@utu.fi
Submitted 2015-01-10. Accepted 2015-05-21.

Background and purpose — Selective androgen receptor modulators (SARMs) have been developed to have systemic anabolic effects on bones and muscles without the adverse effects of steroidal androgens. One unexplored therapeutic option is the targeted application of SARMs for the enhancement of local new bone formation. We evaluated the osteogenic efficacy of a locally released SARM (ORM-11984).

Methods — ORM-11984 was mixed with a copolymer of L-lactide and ε-caprolactone (PLCL). An in vitro dissolution test confirmed the sustainable release of ORM-11984 from the matrix. A bone marrow ablation model was used in female Sprague-Dawley rats. Implants containing 10%, 30%, or 50% ORM-11984 by weight or pure PLCL were inserted into the medullary canal of the ablated tibia. At 6 and 12 weeks, the volume of intramedullary new bone and the perimeter of bone-implant contact were measured by micro-computed tomography and histomorphometry.

Results — Contrary to our hypothesis, there was a negative correlation between the amount of new bone around the implant and the dose of ORM-11984. There was only a mild (and not statistically significant) enhancement of bone formation in ablated bones subjected to the lowest dose of the SARM (10%).

Interpretation — This study suggests that intramedullary/endosteal osteogenesis had a negative, dose-dependent response to locally released SARM. This result highlights the complexity of androgenic effects on bones and also suggests that there are biological limits to the targeted local application of SARMs.

Male and female hormones, which act mainly via androgen receptors (ARs) and estrogen receptors (ERs), are physiological regulators of bone remodeling (Clarke and Khosla 2009, Vanderschueren et al. 2014). Drug development programs have successfully launched non-steroidal selective estrogen receptor modulators (SERMs) for various clinical indications, including postmenopausal osteoporosis (Komm and Mirkin 2014). The common goal of the corresponding programs for non-steroidal tissue-selective androgen receptor modulators (SARMs), which act as AR ligands, is to achieve systemic anabolic effects on bones and muscles without adverse androgenic effects (Mohler et al. 2009). Preclinical models have shown that the systemic administration of SARMs can protect the skeleton from the catabolic effects of orchiectomy and ovariectomy (Gao et al. 2005, Kearbey et al. 2007), partially restore the bone mass lost by ovariectomy (Kearbey et al. 2009), and enhance the therapeutic effects of anti-resorptive drug treatment (Vajda et al. 2009). The main clinical target of SARMs is aging populations with sarcopenia and bone frailty (Mohler et al. 2009), but no SARMs have yet reached the market.

ARs are highly expressed in mature osteoblasts and osteocytes (Abu et al. 1997, Wiren et al. 2002), and androgens have been traditionally claimed to have direct anabolic bone effects. Data from studies on androgen-insensitive null mice with non-functional ARs (Yeh et al. 2002, Kawano et al. 2003, Venken et al. 2006, Sinnesael et al. 2012) and in mice that overexpress ARs (Wiren et al. 2004, 2008) have confirmed the physiological significance of AR-mediated bone remodeling processes. The androgenic action may be partly compartment-specific, and anabolic effects mainly appear at periosteal surfaces (Wiren et al. 2004, 2008, 2010, 2011), but several studies have clearly demonstrated that the lack of AR action results in general trabecular bone loss (Vanderschueren et al. 2014).

Clinically, there are unmet needs for bone enhancement agents in elective reconstructive procedures and also in trauma surgery. One unexplored therapeutic option would be local application of SARMs as an anabolic bone agent. In this pilot study, the osteogenic efficacy of a SARM compound (ORM-11984) was tested in a rat bone marrow ablation model. Bone marrow ablation is a unique bone-healing model in which

DOI 10.3109/17453674.2015.1074840

robust endosteal intramembranous bone formation is induced transiently by surgical ablation of the bone marrow (Suva et al. 1993). ARs are present in mesenchymal stromal stem cells of the bone marrow (Bellido et al. 1995), which are among the repair cells responsible for bone-healing processes (Bais et al. 2009). We hypothesized that the intramedullary administration of ORM-11984 would have androgenic anabolic effects on bone marrow-derived precursor cells and produce a dose-dependent enhancement of the local osteogenic response.

Material and methods

Preparation of the implants and dissolution test

ORM-11984 is a non-steroidal AR agonist, the result of a drug development program (Orion Corporation, Turku, Finland). In line with preclinical results from other SARMs, ORM-11984 has been shown to prevent osteopenia in rat models of ovariectomy and orchidectomy, and to enhance the therapeutic effects of alendronate in the same rat orchidectomy model (unpublished data).

ORM-11984 was incorporated in a biodegradable polymer matrix to act as a controlled drug delivery system. A commercially available copolymer of L-lactide and ε-caprolactone (PLCL) with the co-monomer L/C ratio of 70/30 (PURASORB PLC 7015; Purac Biomaterials, Gorinchem, the Netherlands) was loaded with different doses of ORM-11984 (10%, 30%, or 50% by weight, corresponding to target doses of 1.06 mg, 3.19 mg, and 5.21 mg ORM-11984). ORM-11984 was embedded in the matrix by mixing it with the polymer melt. It dissolved into the molten polymer uniformly. The inherent viscosity of the polymer is 1.5 dL/g, and in a biological environment it degrades within 12–24 months. The extrudate was cut into small billets (length 5 mm, diameter 1 mm) and packed in glass vials for sterilization by gamma irradiation.

An in vitro dissolution test was performed to study the rate of release of 6 mg ORM-11984 from samples containing 10%, 30%, or 50% of the compound by weight. The sample of the 10% group contained 6 implants, the sample of the 30% group contained 2 implants, and the sample of the 50% group contained one implant. The samples were immersed in 500 mL phosphate buffer (pH 6.8) for 14 days. The solution was paddled at 100 rpm up to day 9 and at 200 rpm from day 9 onwards. The release of ORM-11984 from the samples was measured daily by spectrophotometry at a wavelength of 268 nm using fiber optics with a 10-mm light path. The baseline measurement was obtained at wavelengths of 350–375 nm.

Animals

We used female Sprague-Dawley rats from Harlan Netherlands B.V. (age 15–19 weeks, weight 267–310 grams). The study plan included 42 animals (Table 1). 5 animals did not recover from the anesthesia, and they were replaced.

Table 1. Experimental groups, implant compositions, and group sizes for each time point

Group	Implant composition	Time point 6 / 12 weeks n / n
Placebo control	PLCL 100%	5 / 5
10% ORM-11984	ORM-11984 10% + PLCL 90%	4 / 4
30% ORM-11984	ORM-11984 30% + PLCL 70%	4 / 4
50% ORM-11984	ORM-11984 50% + PLCL 50%	4 / 4
Negative control	No implant	4 / 4

Design

A bone marrow ablation model of the rat tibia (Välimäki et al. 2006) was used. 2 implants were inserted into the left tibia of each animal. The animals were randomized into 5 groups according to the type of implant inserted (Table 1). The 3 ORM-11984 groups received 2 implants containing 10%, 30%, or 50% ORM-11984 by weight. The placebo control group received 2 implants, composed of pure PLCL polymer. In the negative control group, the medullary cavity was left unfilled after marrow ablation. The amount of intramedullary new bone at 6 weeks was measured as the primary outcome. The maintenance of the newly formed bone at 12 weeks was evaluated as the secondary outcome. The amount of intramedullary new bone was measured volumetrically by microcomputed tomography (μCT). The μCT data were also applied to the measurements of the cortical bone dimensions and the volumetric mineral density measurements. The bone samples retrieved were processed for histomorphometric measurement of the areas of the new bone around the implant and its contact with the implant. A schematic illustration of the surgical model and the analyses is given in Figure 1.

Methods

Anesthesia and medication. The animals were anesthetized with subcutaneous administration of a mixture of ketamine hydrochloride and medetomidine. Standard postoperative pain medication (buprenorphine) was given subcutaneously for 3 days after surgery.

Surgery. Standard aseptic conditions were used. The proximal metaphyseal area of the left tibia was approached. Using a high-speed dental drill, a round cortical defect ("cortical window", 2.8 mm in diameter) was made under saline irrigation in the anteromedial cortex of the proximal tibia below the insertion of the medial collateral ligament. A smaller cortical defect ("vent", 1.0 mm in diameter) was drilled 5 mm distal to the "cortical window" (Figure 1). The bone marrow of the medullary space in the region of the cortical window and the vent was removed by rinsing with 0.9% saline solution. After marrow ablation, the 2 sterile implants were inserted into the medullary canal according to the order of the randomization list. The 2 implants were used instead of one due to technical

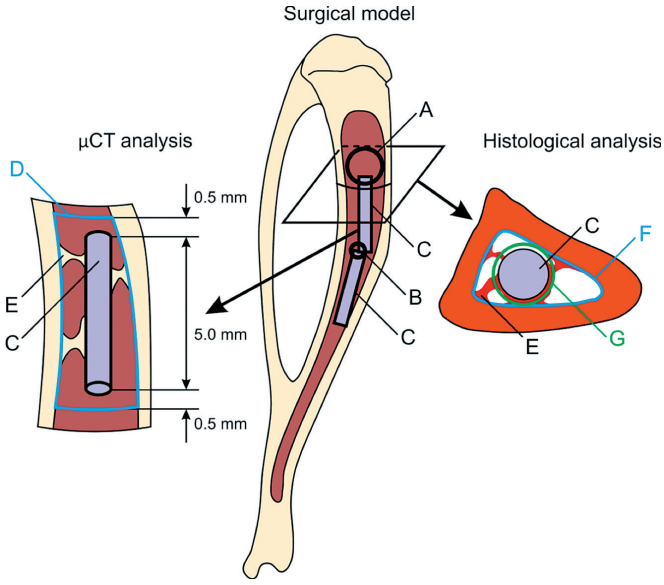

Figure 1. The surgical model and analyses of peri-implant bone formation. Bone marrow ablation was performed through the proximal cortical window (panel A) and the distal vent (B). 2 implants (C) were inserted into the medullary canal. In the μCT analysis, the volume of interest (VOI) (D) was constructed by outlining the endosteal border of the cortex on the cross-sectional images. It was bordered 0.5 mm proximal to and 0.5 mm distal to the ends of the implant (C). The volume of newly formed bone (E) was measured inside the VOI with the volume of the implant deducted. In the histological analysis, the region of interest (ROI 1) was constructed by outlining the endosteal border of the cortex (F). The area of newly formed bone (E) was evaluated inside ROI 1 with the area of the implant (C) deducted. The peri-implant region of interest (ROI 2) was constructed by offsetting the outer border of the implant by 50 μm (G) and deducting the area of the implant (C). The area of peri-implant new bone was evaluated within ROI 2.

difficulties in insertion of one long implant. The piece of cortical bone was reinserted into the cortical window, and the soft tissues were closed in layers.

Follow-up. After recovery from the anesthesia, animals had free access to water and food. Animals were closely monitored for uneventful recovery and any local complications. Free unrestricted weight bearing was allowed.

Killing. At 6 and 12 weeks, the animals were killed by decapitation under CO2 narcosis. The operated tibias were harvested for the analyses.

Analysis

Micro-computed tomography. The retrieved tibias were scanned with a Skyscan 1072 μCT system (Skyscan NV, Kontich, Belgium). The samples were imaged with a step angle of 0.45º within the full angle of 180º. The shadow projection images obtained at each step angle were reconstructed into a 3-D cross-sectional image stack using NRecon software (Skyscan) with an isotropic voxel size of 8.23 μm. The image stacks were analyzed using CTAn software (Skyscan). In the analysis, a volume of interest (VOI) was constructed by outlining the endosteal border of the cortex on the cross-sectional images using a standardized step of 1 mm between the images. The VOI delimited the intramedullary volume 0.5 mm proximal to and 0.5 mm distal to the ends of the proximal implant, as shown in Figure 1. In the analysis, the newly formed bone was segmented from the bone marrow using a global thresholding technique. The volume of the implant was deducted from the VOI.

The μCT data were applied to the measurements of the cortical bone dimensions. To calculate the equivalent endosteal radius, the original intramedullary VOI was approximated by a cylinder of the same volume and height. For measurement of cortical thickness, the original intramedullary VOI was programmatically dilated to the periosteal border of the cortex in the cross-sectional image planes, and this served as the periosteal VOI. The equivalent periosteal radius was calculated for the periosteal VOI. The thickness of the cortex was calculated as the difference between the equivalent periosteal radius and the equivalent endosteal radius.

Measurements of the volumetric tissue mineral density (TMD) were performed from the μCT data. The TMD was calculated from the voxels segmented to represent bone tissue (Bouxsein et al. 2010). 2 hydroxyapatite phantoms (250 and 750 mg/cm3), which were provided by the manufacturer of the μCT scanner, were imaged adjacent to the tibias. The phantoms were used to convert the attenuation values obtained in the imaging to the density values. The density of the newly formed intramedullary bone was measured within the intramedullary VOI. The cortical density was measured in the cortical VOI obtained by subtraction of the intramedullary VOI from the periosteal VOI.

Histomorphometry. The bone specimens were dehydrated in a graded ethanol series and embedded, without decalcification, in isobornyl methacrylate (Technovit 7200 VLC; Heraeus Kulzer GmbH & Co. KG, Wehrheim, Germany) as previously described (Välimäki et al. 2006). Cross sections of 10- to 20-μm thickness, perpendicular to the long axis, were obtained from the tibias using a cutting and grinding system (Exakt-Apparatebau, Hamburg, Germany).

The sections were stained with the van Gieson method and imaged with a virtual microscope (Olympus BX51TF; Olympus Corp., Tokyo, Japan) controlled by special software (dotSlide 1.2; Olympus Soft Imaging Solutions GmbH, Münster, Germany). One section cut in the middle of the proximal implant was used for the histomorphometric analysis of the new bone around the implant and its contact with the implant. The amount of new bone formed in the ablated canal around the implant was measured using CTAn software (Skyscan). Based on the set-up (Figure 1), the region of interest (ROI 1) was constructed by outlining the endosteal border of the cortex. In the analysis, the new bone was segmented from the bone marrow using a global thresholding technique, and the area of the implant was deducted from ROI 1. The area of new bone on the section was measured, expressed as a percentage of the cross-sectional area of the intramedullary canal,

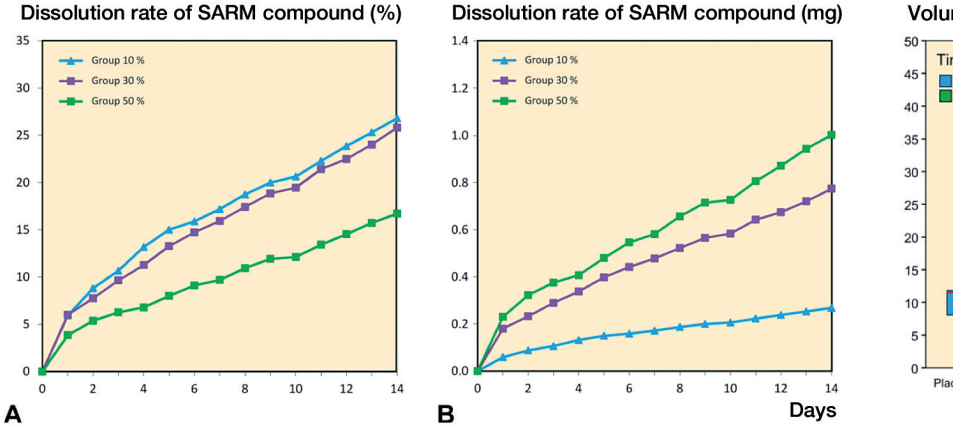

Figure 2. The release rate of ORM-11984 from the PLCL implants containing 10%, 30%, or 50% of the compound (by weight). The in vitro dissolution test had a fixed ORM-11984 dose of 6 mg. This dose required the immersion of 6 implants in the 10% group, 2 implants in the 30% group, and one implant in the 50% group (panel A). When the release rate was normalized against the number of immersed implants, the release rate was dependent on the concentration of the compound (B).

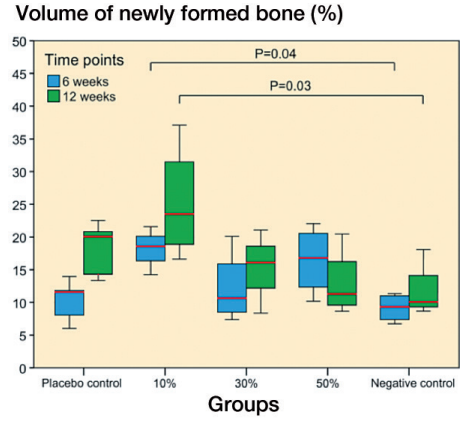

Figure 3. Volumetric µCT analysis of intramedullary new bone showed significant differences between the 3 SARM-treated groups (10%, 30%, or 50% ORM-11984) and the 2 controls at 6 weeks (p = 0.04) and 12 weeks (p = 0.03) (ANOVA with Tukey's post hoc test). In the box plot presentation, the box denotes the first and third quartiles. The horizontal line inside the bar is the median. The whiskers show the range of the data.

and applied as a histomorphometric reference to the volumetric µCT data for new bone. For the assessment of new bone around the implant, a second ROI (ROI 2) was constructed by offsetting the outer border of the implant by 50 µm and deducting the area of the implant. The amount of new bone around the implant was measured and expressed as a percentage of the area of the resultant 50-µm-wide peri-implant ring. The bone-implant contact (BIC), defined as a fraction (%) of the outer perimeter of the implant surface in contact with new bone, was also measured.

Statistics

A power analysis was not possible without having any pre-existing data. Results are presented as mean (SD). Normal distribution of the data was verified using the Kolmogorov-Smirnov test. 1-way ANOVA with Tukey's post hoc t-test was performed to evaluate the primary and secondary outcomes, i.e. the differences in intramedullary new bone between the groups at 6 and 12 weeks, respectively. A non-parametric Spearman rank-order correlation analysis was used to investigate the dose response to the concentrations of SARM and to correlate the results of the µCT and histomorphometric analyses. Statistical significance was assumed at p-values of < 0.05.

Ethics

The animal study protocol was approved by the Finish National Animal Experiment Board (permit ESAVI/1184/04.10.03/2011). The animal experiments were conducted at the Central Animal Laboratory of the University of Turku in accordance with the institutional guidelines for analgesia and anesthesia.

Results

In vitro dissolution test. The release curves of the in vitro dissolution test showed a sustained controlled release of ORM-11984 from the 3 groups of PLCL composite implants containing 10%, 30%, or 50% of the compound (Figure 2A). Reflecting the fixed dose (6 mg of ORM-11984) and the different number of implants immersed, the dissolution rate was slowest in the 50% ORM-11984 group. When the data were normalized against the number of immersed implants, the release was proportional to the concentration of the compound, i.e. lowest in the 10% ORM-11984 group and highest in the 50% ORM-11984 group (Figure 2B).

Intramedullary new bone. Bone marrow ablation combined with the insertion of ORM-11984-loaded implants or pure PLCL implants resulted in intramembranous bone formation. The volume of intramedullary new bone, expressed as a percentage of the VOI, was significantly different between the groups at both 6 weeks ($p = 0.02$, ANOVA) and 12 weeks ($p = 0.03$, ANOVA) (Figure 3). At 6 weeks, the 10% ORM-11984 group showed a significant difference compared to the negative control group ($p = 0.04$) and a higher new volume than the placebo group ($p = 0.06$). At 12 weeks, there was a significant difference between the 10% ORM-11984 group and the negative control group ($p = 0.03$), and the 10% ORM-11984 group also showed a higher new bone volume than the 50% ORM-11984 group ($p = 0.05$). The Spearman rank-order correlation analysis showed a negative correlation ($r_s = -0.43$; $p = 0.09$) between the volume of intramedullary new bone and the dose of ORM-11984 at 12 weeks. The volumetric measurement of intramedullary new bone showed a correlation with the histomorphometric data of intramedullary new bone measured on one plane ($r_s = 0.73$; $p < 0.001$). There were no statistically

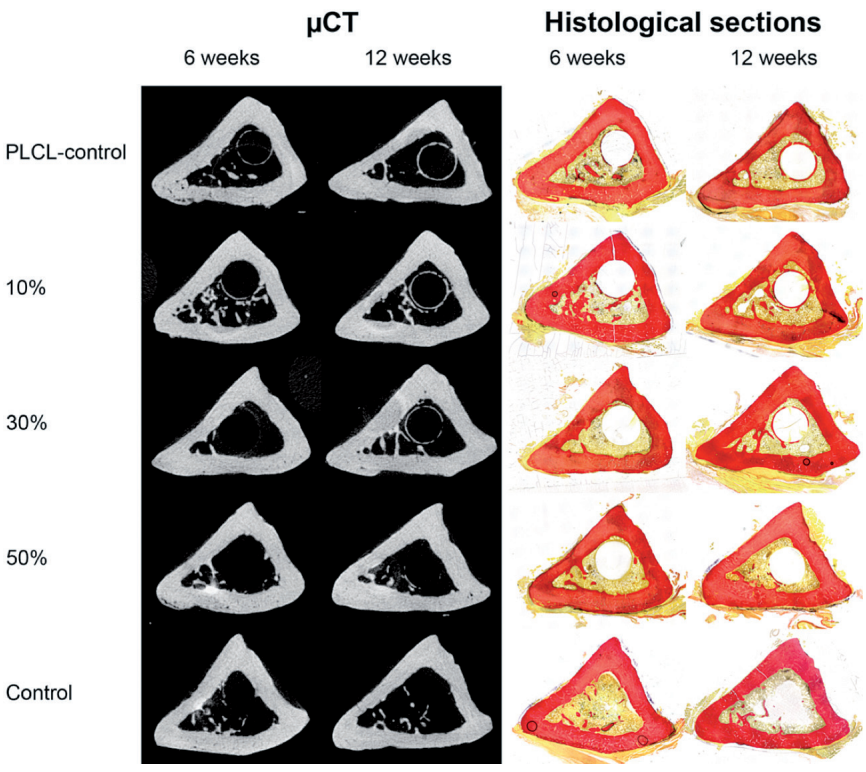

Figure 4. Cross-sectional μCT images and histological sections (van Gieson stain) of rat tibias 6 and 12 weeks after bone marrow ablation and the implantation of polymer (PLCL) implants loaded with 10%, 30%, or 50% ORM-11984. There were 2 control groups: the placebo control (pure PLCL) and the negative control (ablation only).

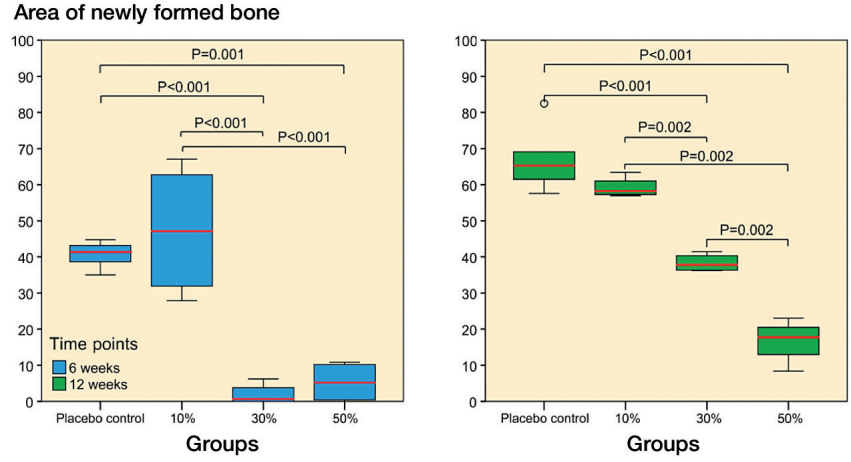

Figure 5. Histomorphometric analysis of new bone in the 50-μm peri-implant ring showed significant differences (ANOVA with Tukey's post hoc test) between the placebo group and the 3 SARM-treated groups at 6 and 12 weeks (10%, 30%, or 50% ORM-11984). The box plot presentation is explained in Figure 3.

significant inter-group differences in the volumetric TMD of intramedullary new bone (Table 2, see Supplementary data).

New bone around the implant. A layer of new bone covered the surfaces of the placebo and 10% ORM-11984 implants (Figure 4). The groups with higher doses of ORM-11984 lacked peri-implant new bone at 6 weeks. The ring of peri-implant new bone became visible in the 30% ORM-11984 group by 12 weeks, whereas the 50% ORM-11984 group still showed very little new bone around the implant. The results of the qualitative evaluation of the μCT images and histological sections were confirmed by histomorphometry of the peri-implant ring area. There were statistically significant differences in the amount of peri-implant new bone between the groups (Figure 5). The 10% ORM-11984 and placebo groups showed no significant inter-group differences in the amount of new bone around the implant, and the amount increased between 6 and 12 weeks in both groups ($p = 0.002$ and $p < 0.001$, respectively). The 30% and 50% ORM-11984 groups showed no or minimal new bone around the implant at 6 weeks ($p \leq 0.001$ compared to the placebo implants). At 12 weeks, the 30% ORM-11984 implants and to a lesser extent the 50% ORM-11984 implants showed a delayed start of new bone formation around the implant, but the difference in the amount was still highly significant ($p < 0.001$ for both groups) compared to the placebo group. The Spearman rank-order correlation analysis showed a significant negative correlation ($p \leq 0.001$) between the dose of ORM-11984 and the area of peri-implant new bone ($r_s = -0.73$ at 6 weeks and $r_s = -0.92$ at 12 weeks).

Bone-implant contact. The lack of new bone around the implant reflected the bone-implant contact (BIC) results in the 30% and 50% ORM-11984 groups. There was no BIC in the 30% ORM-11984 implants at 6 weeks, but the inhibition of BIC was transitory and the group reached the BIC level of the placebo group by 12 weeks. The 50% ORM-11984 group had no BIC at 6 weeks and only a minimal amount of BIC at 12 weeks ($p = 0.001$ compared to the placebo group). The amount of BIC stayed at a constant level (approximately 40%) in the placebo group and the 10% ORM-11984 group between 6 and 12 weeks (Figure 6), although the amount of new bone increased around these implants. The Spearman rank-order correlation analysis showed a negative correlation ($p < 0.001$) between the dose of ORM-11984 and the BIC ($r_s = -0.70$ at 6 weeks and $r_s = -0.75$ at 12 weeks).

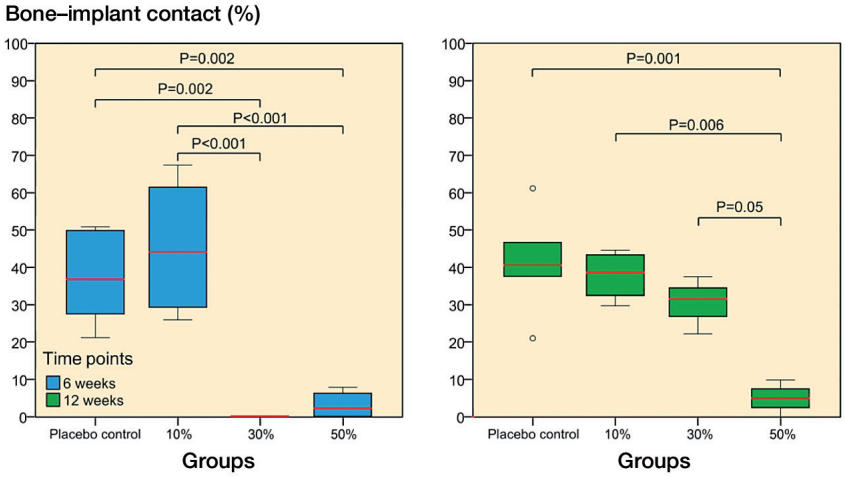

Figure 6. Histomorphometric analysis of bone-implant contact (BIC) showed significant differences (ANOVA with Tukey's post hoc test) between the placebo group and the 3 SARM-treated groups at 6 and 12 weeks (10%, 30%, or 50% ORM-11984). The box plot presentation is explained in Figure 3.

Cortical bone dimensions. The measurements of the equivalent periosteal radius and endosteal radius showed no significant inter-group differences (Table 3, see Supplementary data). Only the 10% ORM-11984 group showed a temporary increase in the periosteal radius at 6 weeks ($p = 0.07$). The calculation of cortical thickness showed no significant inter-group differences at 6 weeks (Table 3, see Supplementary data), but at 12 weeks the 10% ORM-11984 group showed a diminished cortical thickness (591 (SD 40) µm) compared to the negative control group (656 (SD 29); $p = 0.03$) and the 30% ORM-11984 group (648 (SD 30); $p = 0.05$). As a measure of the cortical bone quality, there were no significant differences between the ORM-11984 groups and the controls in the volumetric TMD of the cortical bone (Table 2, see Supplementary data).

Discussion

The present study was designed to evaluate the efficacy of a locally released SARM compound in the promotion of intramedullary osteogenesis. Contrary to our hypothesis, we observed a dose-dependent suppression of intramedullary/endosteal osteogenesis in response to ORM-11984. The most striking finding was the lack of new bone in the peri-implant ring area of 50 µm and the inhibition of contact with the implant surface. Our methodology did not allow evaluation of the mechanisms underlying the tissue responses observed, but our results appear to be in line with results obtained with transgenic male mice overexpressing ARs, which have shown the same outcome, i.e. inhibition of endocortical bone formation (Wiren et al. 2004, 2008, 2010). Thus, although our results were unexpected, they appear to add one small piece of evidence to the complex nature of the compartment-specific androgenic effects on the skeleton. The increased (although not statistically significantly so) osteogenesis in the 10% ORM-11984 group suggests that a certain controlled level of androgen signaling in female rats may have a minor anabolic effect on intramedullary/endosteal osteogenesis.

The dose-dependent response suggests that the release of ORM-11984 from the PLCL matrix occurred in a controlled manner, confirming the results of the in vitro dissolution test. Biodegradable polymer systems, such as PLCL, are recommended for drug delivery applications for a predefined time span, to target a specific tissue (Pitt et al. 1979). The slowest release from the 50% ORM-11984 group was probably related to differences in the total surface area of the immersed implants. Another possibility is that a high dose of ORM-11984 results in re-crystallization within the chains of the matrix polymer, which would limit the dissolvability of the compound. Nevertheless, when the data were normalized against the number of implants, the expected concentration-dependent release of ORM-11984 was observed.

The application of the bone marrow ablation model provided standardized bone-healing conditions at a well-defined anatomic site for estimation of the biological response to local SARM treatment. Mesenchymal stromal stem cells of the bone marrow, which express ARs (Bellido et al. 1995), are among the key bone repair cells (Bais et al. 2009) and are therefore the ideal target for testing of the capacity of a SARM in the enhancement of local osteogenesis. Surgical bone marrow ablation is a trigger for the phase of rapid intramembranous osteogenesis within 1 week, followed by a synchronized sequence of complete osteoclastic resorption of the newly formed bone within 2 weeks (Suva et al. 1993). The model has been shown to be a preferential technique for investigation of anabolic bone drugs (Zhang et al. 2010). Based on our previous results using the model on bioactive glass microspheres (Välimäki et al. 2006), the strongest osteogenic response was expected to be observed between 4 and 8 weeks. Thus, we selected the time point of 6 weeks for evaluation of the primary efficacy of ORM-11984. Based on extrapolation of the in vitro release profiles, the main excretion of the ORM-11984 doses loaded was estimated to last a minimum of 3 months. Thus, the 12-week time point was selected to evaluate the maintenance of the newly formed bone under continued exposure to the SARM. Based on rabbit studies on the osteoconductivity of polylactide composites (Daculsi et al. 2011), the slowly resorbing PLCL matrix was expected to temporarily induce contact osteogenesis and show a zone of new bone surrounding the implant surface. Indeed, this type of new bone was constantly observed around and in contact with the pure PLCL implants.

Our goal was to determine the response of mesenchymal stromal stem cells from the bone marrow to the SARM under normal bone-healing conditions. Thus, the experiment focused on adult female rats without ovariectomy. We selected this animal model as the most sensitive option to prove or disprove the anabolic effects of the SARM on bone marrow-derived precursor cells. Female rats have a physiologically low level of androgens, creating a minimum amount of competition with the locally applied SARM, and these present normal levels of estrogens for the maintenance of an undisturbed bone-healing response. There may be a tendency of higher expression of AR in male rats than in female rats (van der Eerden et al. 2002), but it is a common belief that sex-related skeletal differences mainly reflect physiological differences in the levels of circulating female and male hormones. Transgenic mouse models have demonstrated that skeletal changes caused by the overexpression of ARs (Wiren et al. 2004, 2008) or inactivation of ARs (Yeh et al. 2002, Kawano et al. 2003) are observed predominantly or entirely in male AR- transgenic mice, due to higher circulating androgen levels. In the current experiment, the expression of ARs in the responding cells was not manipulated, but ORM-11984, acting as an AR ligand, was locally applied to artificially enhance the physiological androgenic effects on the responding osteogenic bone marrow cells. Under these conditions, the presence of high levels of circulating androgens (i.e. male sex) could have overshadowed the effect of the SARM selected. In contrast, estrogen deficiency caused by surgical ovariectomy (i.e. simulation of the postmenopausal state) may have impaired the bone-healing capacity (Hatano et al. 2004) and increased the physiological AR-mediated effects of circulating androgens. It must be emphasized that the therapeutic efficacy of a systemic SARM treatment is unquestionable in female rats. Different SARMs (Kearbey et al. 2007, 2009, Vajda et al. 2009), including ORM-11984, can prevent bone loss caused by ovariectomy and even restore bone mass in ovariectomized rats with established osteopenia.

One might speculate that the reduced amount of new bone around the implant that we observed in the marrow ablation model was a result of a supra-physiological dosing of the SARM selected. It is well recognized that local dosing of bone enhancement agents, such as selection of the carrier for BMPs (Seeherman et al. 2012), is demanding. For example, rhBMP-2 clinical trials have not uniformly achieved the success expected (Aro et al. 2011), and it has been claimed that the conflicting results are related to supra-physiological dosing (Hunziker et al. 2012, Kim et al. 2013). However, even a relatively low intraosseous dosing of rhBMP-2 initially induces receptor activator of nuclear factor-κB ligand (RANKL)/osteoprotegerin (OPG)-mediated osteoclastic bone resorption followed by stimulation of new bone formation (Seeherman et al. 2010). Interestingly, the molecular mechanism underlying the androgenic suppression of endocortical bone formation appears to be related to altered BMP signaling, which contributes to androgen inhibition of osteoblast differentiation and mineralization (Wiren et al. 2010). Based on the histomorphometric and μCT analyses performed in this study, the dose-dependent inhibition of new bone formation around the implant and also the slow dose-dependent recovery of peri-implant new bone formation suggests that these phenomena were biological responses to the locally released SARM. As discussed, the most likely mechanism is the direct compartment-specific suppression of new bone formation in response to enhanced androgen signaling caused by the SARM. We cannot exclude the possibility that the lack of peri-implant new bone was only secondary to an earlier phase of enhanced bone resorption. Similar to the mechanism of bone resorption induced by rhBMP-2 (Seeherman et al. 2010), undifferentiated marrow stromal cells with a high RANKL/OPG ratio can initiate and support local osteoclastogenesis (Gori et al. 2000). This could be an indirect mechanism of bone resorption if present in SARM-treated bones. It is unlikely that a SARM directly induces osteoclastic resorption. Osteoclasts have ARs (van der Eerden et al. 2002), and androgens inhibit osteoclastic activity (Pederson et al. 1999, Kawano et al. 2003) and osteoclastogenesis (Bellido et al. 1995). Male transgenic mice that overexpress ARs have also shown reduced osteoclastic activity (Wiren et al. 2008), demonstrating the AR-mediated inhibition of bone resorption.

Anabolic PTH treatment has been shown to increase the thickness of cortical bone due to endosteal and periosteal bone formation in a bone marrow ablation model (Zhang et al. 2010). We did not observe such an anabolic response. Only the lowest dose of ORM-11984 (10%) induced a trend of increased osteogenesis and consecutive cortical changes. This sequence of changes was probably true, because none of the other groups showed similar responses. The minor cortical thinning observed could represent a remodeling response to the increased amount of intramedullary new bone. Our previous experimentation of the model has demonstrated that the remodeling of the rat tibia is sensitive to artificially induced formation of new bone in the medullary canal (Välimäki et al. 2006).

Our preclinical experiment was a multidisciplinary academic effort, in collaboration with an industrial partner, to explore the possibility of a new clinical indication for SARMs. The experiment was the first of its type, and forced us to make empirical selections for the study design. As a screening study, the group size was limited, and we tested the effect of ORM-11984 only in the intramedullary/endosteal compartment. The biological response could be different in the periosteal compartment and in metaphyseal regions. Due to the limited number of follow-up time points, we could not evaluate the influence of the SARM on the primary bone response after marrow ablation. The bone marrow ablation model is an excellent tool, but it by no means simulates the highly integrated healing processes of combined endochondral and intramembranous osteogenesis in long-bone fractures, which involve the local

recruitment of undifferentiated and committed precursor cells from multiple lineages and differentiated preosteoblasts and osteoblasts (Bais et al. 2009)—and probably also a systemic recruitment of circulating undifferentiated mesenchymal stem cells (Alm et al. 2010). The dosing of ORM-11984 was based on extrapolations of oral systemic doses (3.0 mg/kg/day) used in previous rat experiments (unpublished data). We cannot rule out the possibility that the higher doses of local SARM resulted in systemic effects of SARMs, affecting the negative feedback regulation of serum sex steroids and thereby reducing systemic sex steroid action. As a limitation, we did not analyze serum levels of sex steroids nor the weights of uteri as a sensitive indicator of estrogen status. There was a trend of enhanced osteogenesis in bones subjected to the lowest dose of ORM-11984, but in this respect, the optimal dosing remained undefined. As a limitation, we did not define the release profile of ORM-11984 in vivo, and we did not measure the local tissue concentrations and androgenic activity of the ORM-11984 released.

In conclusion, the local administration of a selective androgen modulator failed to produce a dose-dependent osteogenic response in a rat bone marrow ablation model. There was a negative dose-dependent correlation between the amount of new bone around the implant and the dose of SARM loaded. A similar negative effect was found at the bone-implant contact. The underlying mechanism or mechanisms remain open to speculation, but the results support the concept of complex compartment-specific androgenic effects on the skeleton.

Supplementary data

Tables 2 and 3 are available on the Acta Orthopaedica website, www.actaorthop.org, identification number 8481.

HA: planning of the study, and writing and revision of the manuscript. JK: μ-CT imaging of bone specimens, analysis of μ-CT data, histological and histomorphometrical analysis of bone sections, participation in the statistical analysis, and writing and revision of the manuscript. NM: participation in planning of the study, participation in μ-CT, histological and histomorphometrical analysis, statistical analysis, and writing and revision of the manuscript. EK: participation in planning of the study, and animal surgery. RM: participation in the animal surgery and retrieval of the bone specimens.

This work was supported by Orion Corporation, Finland. The sponsor was not involved in the data analysis. JK is a PhD student in the National Doctoral Programme of Musculoskeletal Disorders and Biomaterials (TBDP) in Finland.

Abu E O, Horner A, Kusec V, Triffitt J T, Compston J E. The localization of androgen receptors in human bone. J Clin Endocrinol Metab 1997; 82 (10): 3493-7.

Alm J J, Koivu HM, Heino T J, Hentunen T A, Laitinen S, Aro H T. Circulating plastic adherent mesenchymal stem cells in aged hip fracture patients. J Orthop Res 2010; 28 (12): 1634-42.

Aro H T, Govender S, Patel A D, Hernigou P, Perera de Gregorio A, Popescu GI, Golden J D, Christensen J, Valentin A. Recombinant human bone morphogenetic protein-2: a randomized trial in open tibial fractures treated with reamed nail fixation. J Bone Joint Surg (Am) 2011; 93 (9): 801-8.

Bais M V, Wigner N, Young M, Toholka R, Graves D T, Morgan E F, Gerstenfeld L C, Einhorn T A. BMP2 is essential for post natal osteogenesis but not for recruitment of osteogenic stem cells. Bone 2009; 45 (2): 254-66.

Bellido T, Jilka R L, Boyce B F, Girasole G, Broxmeyer H, Dalrymple S A, Murray R, Manolagas S C. Regulation of interleukin-6, osteoclastogenesis, and bone mass by androgens. The role of the androgen receptor. J Clin Invest 1995; 95 (6): 2886-95.

Bouxsein M L, Boyd S K, Christiansen B A, Guldberg R E, Jepsen K J, Müller R. Guidelines for assessment of bone microstructure in rodents using micro-computed tomography. J Bone Miner Res 2010; 25 (7): 1468-86.

Clarke B L, Khosla S. Androgens and bone. Steroids 2009; 74 (3): 296-305.

Daculsi G, Goyenvalle E, Cognet R, Aguado E, Suokas E O. Osteoconductive properties of poly(96L/4D-lactide)/beta-tricalcium phosphate in long term animal model. Biomaterials 2011; 32 (12): 3166-77.

Gao W, Reiser P J, Coss C C, Phelps M A, Kearbey J D, Miller D D, Dalton J T. Selective androgen receptor modulator treatment improves muscle strength and body composition and prevents bone loss in orchidectomized rats. Endocrinology 2005; 146 (11): 4887-97.

Gori F, Hofbauer L C, Dunstan C R, Spelsberg T C, Khosla S, Riggs B L. The expression of osteoprotegerin and RANK ligand and the support of osteoclast formation by stromal- osteoblast lineage cells is developmentally regulated. Endocrinology 2000; 141 (12): 4768-76.

Hatano H, Siegel H J, Yamagiwa H, Bronk J T, Turner R T, Bolander M E, Sarkar G. Identification of estrogen-regulated genes during fracture healing, using DNA microarray. J Bone Miner Metab 2004; 22 (3): 224-35.

Hunziker E B, Enggist L, Küffer A, Buser D, Liu Y. Osseointegration: the slow delivery of BMP-2 enhances osteoinductivity. Bone 2012; 51 (1): 98-106.

Kawano H, Sato T, Yamada T, Matsumoto T, Sekine K, Watanabe T, Nakamura T, Fukuda T, Yoshimura K, Yoshizawa T, Aihara K, Yamamoto Y, Nakamichi Y, Metzger D, Chambon P, Nakamura K, Kawaguchi H, Kato S. Suppressive function of androgen receptor in bone resorption. Proc Natl Acad Sci USA 2003; 100 (16): 9416-21.

Kearbey J D, Gao W, Narayanan R, Fisher S J, Wu D, Miller D D, Dalton J T. Selective Androgen Receptor Modulator (SARM) treatment prevents bone loss and reduces body fat in ovariectomized rats. Pharm Res 2007; 24 (2): 328-35.

Kearbey J D, Gao W, Fisher S J, Wu D, Miller D D, Dalton J T. Effects of selective androgen receptor modulator (SARM) treatment in osteopenic female rats. Pharm Res 2009; 26 (11): 2471-7.

Kim H K, Oxendine I, Kamiya N. High-concentration of BMP2 reduces cell proliferation and increases apoptosis via DKK1 and SOST in human primary periosteal cells. Bone 2013; 54 (1): 141-50.

Komm B S, Mirkin S. An overview of current and emerging SERMs. J Steroid Biochem Mol Biol 2014; 143C: 207-22.

Mohler M L, Bohl C E, Jones A, Coss C C, Narayanan R, He Y, Hwang D J, Dalton J T, Miller D D. Nonsteroidal selective androgen receptor modulators (SARMs): dissociating the anabolic and androgenic activities of the androgen receptor for therapeutic benefit. J Med Chem 2009; 52 (12): 3597-617.

Pederson L, Kremer M, Judd J, Pascoe D, Spelsberg T C, Riggs B L, Oursler M J. Androgens regulate bone resorption activity of isolated osteoclasts in vitro. Proc Natl Acad Sci USA 1999; 96 (2): 505-10.

Pitt C G, Jeffcoat A R, Zweidinger R A, Schindler A. Sustained drug delivery systems. I. The permeability of poly(epsilon-caprolactone), poly(DL-lactic acid), and their copolymers. J Biomed Mater Res 1979; 13 (3): 497-507.

Seeherman H J, Li X J, Bouxsein M L, Wozney J M. rhBMP-2 induces transient bone resorption followed by bone formation in a nonhuman primate core-defect model. J Bone Joint Surg (Am) 2010; 92 (2): 411-26.

Seeherman H J, Li X J, Smith E, Wozney J M. rhBMP-2/calcium phosphate matrix induces bone formation while limiting transient bone resorption in a nonhuman primate core defect model. J Bone Joint Surg (Am) 2012; 94 (19): 1765-76.

Sinnesael M, Claessens F, Laurent M, Dubois V, Boonen S, Deboel L, Vanderschueren D. Androgen receptor (AR) in osteocytes is important for the maintenance of male skeletalintegrity: evidence from targeted AR disruption in mouse osteocytes. J Bone Miner Res 2012; 27 (12): 2535-43.

Suva L J, Seedor J G, Endo N, Quartuccio H A, Thompson D D, Bab I, Rodan G A. Pattern of gene expression following rat tibial marrow ablation. J Bone Miner Res 1993; 8 (3): 379-88.

Vajda E G, Hogue A, Griffiths K N, Chang W Y, Burnett K, Chen Y, Marschke K, Mais D E, Pedram B, Shen Y, van Oeveren A, Zhi L, López F J, Meglasson M D. Combination treatment with a selective androgen receptor modulator q(SARM) and a bisphosphonate has additive effects in osteopenic female rats. J Bone Miner Res 2009; 24 (2): 231-40.

Van der Eerden B C, van Til N P, Brinkmann A O, Lowik C W, Wit J M, Karperien M. Gender differences in expression of androgen receptor in tibial growth plate and metaphyseal bone of the rat. Bone 2002; 30 (6): 891-6.

Vanderschueren D, Laurent M R, Claessens F, Gielen E, Lagerquist M K, Vandenput L, Börjesson A E, Ohlsson C. Sex steroid actions in male bone. Endocr Rev 2014; 35 (6): 906-60.

Venken K, De Gendt K, Boonen S, Ophoff J, Bouillon R, Swinnen J V, Verhoeven G, Vanderschueren D. Relative impact of androgen and estrogen receptor activation in the effects of androgens on trabecular and cortical bone in growing male mice: a study in the androgen receptor knockout mouse model. J Bone Miner Res 2006; 21 (4): 576-85.

Wiren K M, Chapman Evans A, Zhang X W. Osteoblast differentiation influences androgen and estrogen receptor-alpha and -beta expression. J Endocrinol 2002; 175 (3): 683-94.

Wiren K M, Zhang X W, Toombs A R, Kasparcova V, Gentile M A, Harada S, Jepsen K J. Targeted overexpression of androgen receptor in osteoblasts: unexpected complex bone phenotype in growing animals. Endocrinology 2004; 145 (7): 3507-22.

Wiren K M, Semirale A A, Zhang X W, Woo A, Tommasini S M, Price C, Schaffler M B, Jepsen K J. Targeting of androgen receptor in bone reveals a lack of androgen anabolic action and inhibition of osteogenesis: a model for compartment-specific androgen action in the skeleton. Bone 2008; 43 (3): 440-51.

Wiren K M, Semirale A A, Hashimoto J G, Zhang X W. Signaling pathways implicated in androgen regulation of endocortical bone. Bone 2010; 46 (3): 710-23.

Wiren K M, Hashimoto J G, Semirale A A, Zhang X W. Bone vs. fat: embryonic origin of progenitors determines response to androgen in adipocytes and osteoblasts. Bone 2011; 49 (4): 662-72.

Välimäki V V, Moritz N, Yrjans J J, Vuorio E, Aro H T. Effect of zoledronic acid on incorporation of a bioceramic bone graft substitute. Bone 2006; 38 (3): 432-43.

Yeh S, Tsai M, Xu Q, Mu X, Lardy H, Huang K E, Lin H, Yeh S D, Altuwaijri S, Zhou X, Xing L, Boyce B F, Hung M C, Zhang S, Gan L, Chang C. Generation and characterization of androgen receptor knockout (ARKO) mice: an in vivo model for the study of androgen functions in selective tissues. Proc Natl Acad Sci USA 2002; 99 (21): 13498-503.